*Semarak Engineering Journal* 7, Issue 1 (2024) 11-30

Semarak Engineering Journal

Journal homepage:
https://semarakilmu.com.my/journals/index.php/sem_eng/index
ISSN: 3036-0145


# The Importance of Adopting Response Surface Methodology to Optimize the Flow and Heat Transfer of Carbon Nanotube Nanofluid over a Stretching or Shrinking Sheet

Nazrul Azlan Abdul Samat[1,2,*], Norfifah Bachok[1,3], Norihan Md Arifin[1,3], Ion Pop[4]

[1] Department of Mathematics and Statistics, Faculty of Science, Universiti Putra Malaysia, 43400 Serdang, Selangor, Malaysia
[2] Department of Management, Faculty of Management and Information Technology, Universiti Sultan Azlan Shah, 33000 Kuala Kangsar, Perak, Malaysia
[3] Institute for Mathematical Research, Universiti Putra Malaysia, 43400 Serdang, Selangor, Malaysia
[4] Department of Mathematics, Babes-Bolyai University, 400084 Cluj-Napoca, Romania

**ARTICLE INFO**

***Article history:***
Received 2 September 2024
Received in revised form 9 October 2024
Accepted 13 November 2024
Available online 15 December 2024

***Keywords:***
CNT nanofluid; heat transfer; MHD; stretching/shrinking sheet; numerical method; RSM

**ABSTRACT**

The research investigates the boundary layer flow and heat transfer of carbon nanotube (CNT) nanofluid over a stretching/shrinking sheet with the magnetohydrodynamic (MHD) effect. The purpose of constructing this model is to increase the understanding of CNT nanofluid flow and heat transfer characteristics since numerous models use metallic nanoparticles. We conduct this study using numerical and response surface methodology (RSM) approaches in MATLAB and Minitab, respectively. We formulate the mathematical formula by applying the non-linear partial differential equations (PDE). Next, we transform the PDE into non-dimensional ordinary differential equations (ODE) by exploiting the similarity variables method. We show that the model produces multiple solutions in the shrinking region. The magnetic parameter can widen the solutions and delay the boundary layer separation. Both numerical and RSM methods reveal that the maximum value of the magnetic parameter maximizes the heat transfer coefficient. Additionally, both methods demonstrate that single-walled CNT nanofluid is better than multi-walled CNT nanofluid in transmitting heat.

## 1. Introduction

Research into optimizing heat transmission through nanofluids has greatly increased over the past five years. Our current understanding indicates that the optimization of heat transport in nanofluids has predominantly emphasized experimental studies compared to numerical data. Due to the challenges in visualizing heat transfer profiles through laboratory trials, the optimization process for heat transfer has transitioned to manipulating numerical simulations. In order to optimize the numerical results of heat transfer in nanofluid characteristics, researchers have utilized several

* *Corresponding author.*
*E-mail address: ilmulight.86@gmail.com*

https://doi.org/10.37934/sej.7.1.1130

prediction models, including response surface methodology (RSM) and artificial neural networks (ANN).

RSM is a robust technique for optimizing responses by integrating multiple factors or inputs using both mathematical and statistical analysis. As RSM is a critical tool to optimize and improve experimental designs, scientists such as Najiyah *et al.*, Mehmood *et al.*, Sheikh *et al.*, and Najiyah *et al.,* [1-4], have employed RSM to optimize the heat transfer characteristics of nanofluids across various geometries and effects. The quadratic regression model can be utilized to attain the optimal response point, specifically for heat transfer coefficients. Multiple studies and reviews, including those by Regi *et al.,* and Kim *et al.,* [5,6], have demonstrated that RSM delivers plenty of benefits for experimental design in optimization, as this method can be executed with a few and limited number of experimental trials. Despite offering diverse advantages, RSM also has some limitations, especially when we want to investigate beyond the range of evaluation factors. This is because, RSM has primarily focused on local analysis, as stated by Veza *et al.,* [7].

Nanofluid, a powerful medium, acts as an engineered fluid to increase the rate of heat transfer through several devices. Akaje and Olajuwon, Samat *et al.*, and Yahaya *et al.,* [8-10] are among the most recent researchers investigating nanofluids. But research on nanofluids continues to exhibit empirical gaps, as Merkin *et al.,* [11] assert that this field remains under development. Since the groundbreaking study by Choi and Eastman *et al.,* [12], the number of studies on nanofluid flow and heat transfer capabilities has increased. The notable thermophysical properties, mainly thermal and electrical conductivity, have surpassed typical heat transfer fluids such as water and kerosene. Also, the powerful properties of nanofluid are mostly due to the large surface area of nanoparticles (NP), with copper (Cu) and aluminum oxide ($Al_2O_3$) becoming the most favorable NP. Sidik *et al.*, Japar *et al.,* Loon *et al.*, and Aziz *et al.,* [13-16] extensively discussed the benefits of using nanofluid in numerous applications. Practically, the preparation of nanofluids which combine NP (with low concentration) and a base water can be done through the single and two-phase methods. Zafar *et al.,* [17] recommended the application of the Tiwari and Das model (single-phase model) to mathematically formulate nanofluid models across various surfaces and physical situations. The suggestion from Zafar *et al.,* [17] is beneficial for further exploration into thermal management systems. However, this team proposed redirecting the selection of NP based on Cu to an alternative possible NP.

Khoswan *et al.,* [18] suggested focusing more on carbon nanotube (CNT) for selecting NP for nanofluid. Afrand *et al.,* [19] had already made this choice because CNT, especially single (SWCNT) and multi (MWCNT)-walled CNT, was found to have the best thermal conductivity compared to other common NP. Despite having excellent thermal physical properties, the number of investigations using both SWCNT and MWCNT is considered low. Given the significant gap in research on CNT nanofluid, it is crucial to extensively formulate nanofluid flow-base CNT nanofluid, which has the potential to enhance nanofluid flow behavior and heat transfer.

The examination of nanofluid flow over stretchable and shrinkable sheets has substantially intensified since Crane's [20] initial study in 1970. According to Swapna *et al.*, [21], a stretching sheet refers to a sheet that moves away from a stagnation point along the $x$-axis. A shrinking sheet can be defined as a movement of a sheet approaching the stagnation point along the $x$-axis. Both of the sheet movements can be displayed in Figure 1. Practically, innovations in nanofluid flow in this context can enhance applications in cooling systems, polymer processing, and the glass extrusion sector. Bachok *et al.*, [22] revealed that stagnation point flow across a stretching/shrinking sheet in nanofluid markedly enhanced the heat transfer process. Yashkun *et al.,* [23] used different kinds of nanofluids, such as copper-water ($Cu$-$H_20$), aluminum-water ($Al_2O_3$-$H_20$), and titanium dioxide-water ($TiO_2$-$H_20$), to show that the suction and slip effects improved the flow of heat along a sheet that could expand and contract. Recently, Mahabaleshwar *et al.,* [24] utilized the combination of black iron oxide and water-based nanofluid ($Fe_3O_4$-$H_20$) to show the efficiency of the thermal process over a stretching sheet under the radiation effect. The research, based on the Casson nanofluid model, revealed that increasing the stretching parameter reduced the velocity profile.

Norzawary *et al*., [25] conducted one of the initial investigations of CNT nanofluid flow and heat transmission over a stretching and shrinking sheet. This team proved that an increased volume fraction of CNT, along with the effect of injection, accelerated flow separation. Furthermore, they observed that the performance of SWCNT surpassed that of MWCNT in terms of both skin friction and heat transfer coefficients. A year later, Mahabaleshwar *et al.,* [26] executed an investigation of CNT flow over a similar surface under the mass transpiration effect. It was shown that the mass transpiration effect made the boundary layer much thicker in both SWCNT and MWCNT nanofluid flows. Recently, Mahabaleshwar *et al.,* [27] completed a study on the flow of CNT through an extending and contracting sheet, accounted for the effects of thermal radiation. Their findings indicated that the velocity and temperature profiles of SWCNT water nanofluid surpassed those of MWCNT water nanofluid.

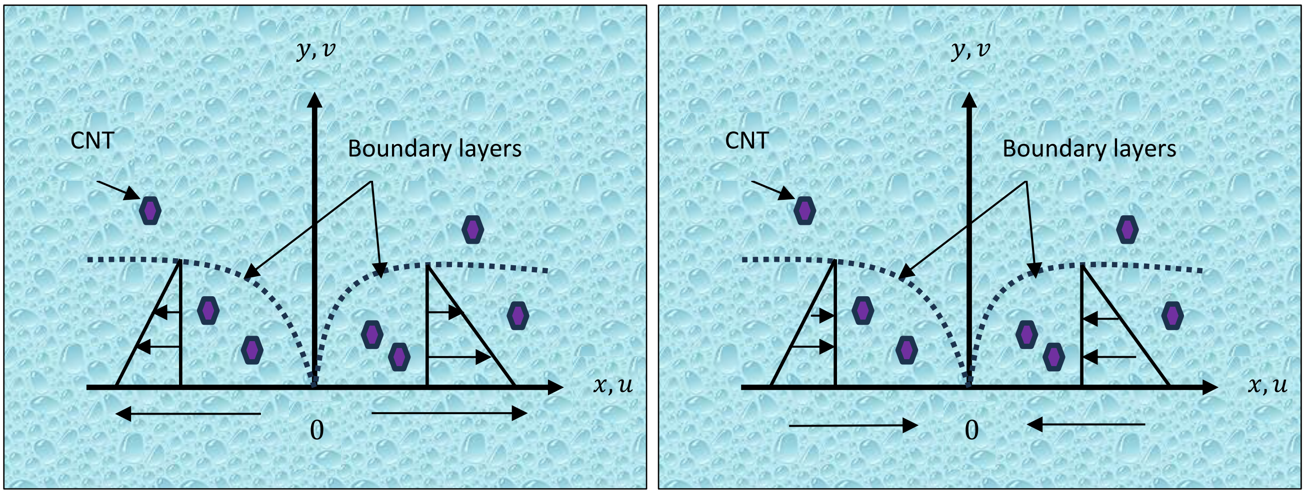


(a) (b)

**Fig. 1.** CNT nanofluid flow over a (a) stretching sheet (b) shrinking sheet

Motivated by the above studies and the potential to contribute to a better understanding of CNT nanofluid flow and heat transfer characteristics, we decided to extend several previously worked studies. The debate over whether SWCNT or MWCNT performs better in heat transfer enhancement also influences our motivation. Samat *et al.,* [28] concluded that SWCNT surpasses MWCNT in heat transfer rate, while Kang *et al*., [29] reported opposing results.

The current model incorporates the influences of the magnetohydrodynamics (MHD) effect. Sahin and Namli [30] reported experimentally that MHD can enhance the heat transfer rate up to 60% due to magnetic field and Lorentz force effects. To the best of our knowledge, the existing research has not yet examined CNT nanofluid motion on a stretching and shrinking plate under both impacts. The gap has created significant opportunities to investigate this effect through numerical and optimization methods. Consequently, by formulating a new mathematical correlation for the magnetic parameter related to the CNT nanofluid, our present study can address a substantial deficiency in prior models. The incorporation of both physical components is crucial for the establishment of predictive models for boundary layer separation. Many devices require flow controllers that have the capability to maintain the laminar phase for an extended duration. In developing the mathematical correlation of the magnetic effect, we take into account the electrical conductivity features of CNT as previously discussed in Jaafar *et al.,* [31]. Numerous models in literature have overlooked the impact of the electrical conductivity characteristics of nanoparticles. We compare the development of previous models with the current model, as shown in Table 1, in order to summarize the gap in boundary layer nanofluid flow over a stretching/shrinking sheet.

**Table 1**
Comparison between previous models and current model

| Model | Nanofluid | CNT | MHD | RSM |
|---|---|---|---|---|
| Bachok *et al.*, [22] | Yes | No | No | No |
| Yashkun *et al.,* [23] | Yes | No | No | No |
| Mahabaleshwar *et al.,* [24] | Yes | Yes | No | No |
| Norzawary *et al.*, [25] | Yes | Yes | No | No |
| Current | Yes | Yes | Yes | Yes |

To enhance the originality of our study, we conduct innovative work by integrating both numerical and RSM methodologies. The significance of the study lies in the potential enhancement of mathematical analysis and engineering interest through the integration of these approaches. To create a comprehensive model, we established the following objectives:

i. To formulate a mathematical model of CNT nanofluid flow and heat transfer over a stretchable and shrinkable sheet under the influence of MHD effect;
ii. To determine the range of solutions for the reduced skin friction, $f''(0)$, and heat transfer, $-\theta'(0)$, coefficients;
iii. To estimate the boundary layer separation resulting from variations in several parameters;
iv. To optimize the heat transfer coefficient due to changes in multiple factors.

## 2. Mathematical Framework
### *2.1 Mathematical Modelling*

We develop the mathematical model for this research using non-linear partial differential equations (PDE). The PDE is formulated based on the subsequent assumptions:

i. The model is based on the Tiwari and Das Model [32] (the single-phase mathematical nanofluid model);
ii. The model is formulated using the two-dimensional (2D) Cartesian coordinate $(x, y)$ system;
iii. The CNT nanofluid motion is under steady, laminar, incompressible, and at stagnation point flow conditions with a constant body sheet temperature;
iv. Two varieties of CNT nanofluids are employed: SWCNT-water and MWCNT-water nanofluids;
v. The velocity $u$, is greater than the velocity $v$, i.e., $u >> v$.

Once the assumptions are established, we express the laminar CNT flow of the boundary layer approximation in PDE forms using the Norzawary *et al.*, Mahabaleshwar *et al.*, and Mahabaleshwar *et al.,* models [25-27] as follows:

$$\frac{\partial u}{\partial x}+\frac{\partial v}{\partial y}=0, \tag{1}$$

$$u\frac{\partial u}{\partial x}+v\frac{\partial v}{\partial y}=\frac{\mu_{Cnf}}{\rho_{Cnf}}\frac{\partial^2 u}{\partial y^2}+U_\infty\frac{dU_\infty}{dx}+\left(\frac{\sigma_{Cnf}}{\rho_{Cnf}}B^2\right)(U_\infty-u) \tag{2}$$

$$u\frac{\partial T}{\partial x}+v\frac{\partial T}{\partial y}=\alpha_{Cnf}\frac{\partial^2 T}{\partial y^2}, \tag{3}$$

where $U_\infty, T, \mu_{Cnf}, \rho_{Cnf}, \sigma_{Cnf}, \rho_{Cnf}, \alpha_{Cnf}, \mu_f$, and $\rho_f$, are the velocity of free stream, CNT nanofluid temperature, dynamic viscosity of CNT nanofluid, density of CNT nanofluid, electrical conductivity of CNT nanofluid, thermal diffusivity of CNT nanofluid, dynamic viscosity of water, and density of water, respectively. The term of the magnetic field, $B$, in Eq. (2) is represented as $B=B_0\sqrt{x}$, (refer to Jaafar *et al.,* and Samat *et al.,* [31-33]) where $B_0$ is a constant of magnetic field strength. Eqs. (1) to (3) are formulated subject to the following boundary conditions:
at $y=0$,

$$u=U_w, v=0, T=T_w, \tag{1}$$

and as $y\to\infty$,

$$u\to U_\infty, T\to T_\infty. \tag{2}$$

The terms $U_w$ (Eq. (4)), $T_w$ (Eq. (4)), and $T_\infty$ (Eq. (5)) illustrate the velocity at the boundary layer, the sheet temperature, and the ambient temperature, respectively. The expression for $U_\infty$ in Eq. (5) is represented linearly as $U_\infty=cx$, where $c$ is a positive constant.

Next, we convert the PDE in Eqs. (1) to (5) into non-dimensional ordinary differential equations (ODE) to simplify them into a practical explanation. We manipulate the following similarity variables to transform PDE into ODE (see Waqar and Pop [34]):

$$\eta=\left(\frac{c}{\nu_f}\right)^{1/2}y, \psi=\sqrt{\nu_f}xf(\eta), T=(T_w-T_\infty)\theta(\eta)+T_\infty, \tag{3}$$

where $\eta$, $\psi$, $f$, $\theta$, $\nu_f=\mu_f/\rho_f$ define as non-dimensional boundary layer thickness, non-dimensional stream function, non-dimensional velocity stream function, non-dimensional temperature function, and the kinematic viscosity of water, respectively. The substitution of Eq. (6) into Eqs. to (1) to (5) successfully satisfies the continuity equation in Eq. (1). Additionally, we generate the following expressions for the transformed momentum and energy equations, along with the boundary conditions:

$$\frac{C_1}{C_2}f'''(\eta)+f''(\eta)f(\eta)+M\big(1-f'(\eta)\big)+1=0, \tag{4}$$

$$\frac{1}{Pr}\frac{C_3}{C_4}\theta''(\eta)+f(\eta)\theta'(\eta)=0, \tag{5}$$

subject to:

at $\eta = 0$,

$$f'(\eta) = \varepsilon, f(\eta) = 0, \theta(\eta) = 1, \tag{6}$$

and as $\eta \to \infty$,

$$f'(\eta) \to 1, \theta(\eta) \to 0, \tag{7}$$

where $\varepsilon$ is a non-dimensional stretching/shrinking parameter. We designate the non-dimensional magnetic parameter, $M = \frac{\sigma_{Cnf}}{\rho_{Cnf}} \frac{B_0^2}{c}$. The terms $C_1$, $C_2$, $C_3$, and $C_4$ are defined as follows:

$$C_1 = \frac{\mu_{Cnf}}{\mu_f}, C_2 = \frac{\rho_{Cnf}}{\rho_f}, C_3 = \frac{k_{Cnf}}{k_f}, C_4 = \frac{(\rho C_p)_{Cnf}}{(\rho C_p)_f}. \tag{8}$$

To complete the discussion on model development, we present the thermal-physical properties of SWCNT, MWCNT, and water, as illustrated in Table 2. In addition, we provide the correlation of SWCNT-water and MWCNT-water nanofluid as depicted in Table 3. In Table 3, the symbol $\phi$ refers to the volume fraction of CNT.

**Table 2**
Thermal physical properties of SWCNT, MWCNT, and water (see Khan *et al.,* and Samat *et al.,* [36,37])

| Property | Nanoparticle | | Base fluid |
|---|---|---|---|
| | SWCNT | MWCNT | Water |
| Density, $\rho$ (kg/m$^3$) | 2600 | 1600 | 997 |
| Specific heat, $C_p$ (J/kg K) | 425 | 796 | 4179 |
| Electrical conductivity, $\sigma$ (S/m) | $1.0 \times 10^8$ | $3.5 \times 10^6$ | $5.0 \times 10^{-2}$ |
| Thermal conductivity, $k$ (W/m K) | 6600 | 3000 | 0.613 |

**Table 3**
Correlations of SWCNT-water and MWCNT-water nanofluids (see Khan *et al.,* and Samat *et al.,* [36,37])

| Properties | Correlations |
|---|---|
| Dynamic viscosity | $\mu_{Cnf} = \frac{\mu_f}{(1-\phi)^{2.5}}$ |
| Density | $\rho_{Cnf} = (1-\phi)\rho_f + \phi\rho_{CNT}$ |
| Heat capacity | $(\rho C_p)_{Cnf} = (1-\phi)(\rho C_p)_f + \phi(\rho C_P)_{CNT}$ |
| Thermal conductivity | $k_{Cnf} = k_f \left( \frac{(1-\phi) + 2\phi \frac{k_{CNT}}{k_{CNT} - k_f} \ln \frac{k_{CNT} + k_f}{2k_f}}{(1-\phi) + 2\phi \frac{k_f}{k_{CNT} - k_f} \ln \frac{k_{CNT} + k_f}{2k_f}} \right)$ |
| Electrical conductivity | $\sigma_{Cnf} = \sigma_f \left( 1 + \frac{3\phi \left( \frac{\sigma_{CNT}}{\sigma_f} - 1 \right)}{\left( \frac{\sigma_{CNT}}{\sigma_f} + 2 - \left( \frac{\sigma_{CNT}}{\sigma_f} - 1 \right) \phi \right)} \right)$ |

Note: The subscription of $CNT$ and $f$ refer to CNT and water, respectively.

*2.2 Physical Quantities*

In this section, we derive the skin friction, $C_f$, and the local Nusselt number (heat transfer coefficient), $Nu_x$, in their simplified versions. Based on Norzawary *et al.*, [25], $C_f$ and $Nu_x$ can be written as follows:

$$C_f = \frac{\tau_w}{\rho_f U^2}, Nu_x = \frac{x q_w}{k_f (T_w - T_\infty)}, \tag{9}$$

where $U = U_w + U_\infty$ is a composite velocity (see Azfal *et al.*, [35]). The terms $\tau_w$ and $q_w$ can be described as below equations as the sheet shear stress and the heat flux, respectively:
at $y = 0$,

$$\tau_w = \mu_{Cnf} \frac{\partial u}{\partial y}, q_w = -k_{nf} \frac{\partial T}{\partial y}. \tag{10}$$

Applying results from Section 2.1, we derive the skin friction and heat transfer coefficients in diminished forms related to the local Reynolds number, $Re_x$, as follows:

$$C_f \sqrt{Re_x} = C_1 f''(0), \frac{Nu_x}{\sqrt{Re_x}} = -C_3 \theta'(0). \tag{11}$$

*2.3 Numerical Procedure*

We solve the model using the bvp4c method in MATLAB version R2022b. Before accomplishing them numerically, we turn the higher-order ODE delineated in Eqs. (7) to (10) into first-order ODE. We organize the first-order ODE in Eqs. (7) to (10) as follows:

$$\begin{aligned} &y(1) = f(\eta), y(2) = f'(\eta), y(3) = f''(\eta), y(4) = \theta(\eta), y(5) = \theta'(\eta), \\ &f'''(\eta) = -\frac{C_2}{C_1}\left(f''(\eta) f(\eta) + M\left(1 - f'(\eta)\right) + 1\right), \\ &\theta''(\eta) = -Pr \frac{C_4}{C_3} f(\eta) \theta'(\eta). \end{aligned} \tag{12}$$

subject to

$$\begin{aligned} &ya(1) - \varepsilon = 0, ya(2) = 0, ya(4) - 1 = 0, \\ &yb(2) - 1 = 0, yb(4) = 0. \end{aligned} \tag{16}$$

The terms $a$ is the boundary conditions near the body sheet, i.e., $\eta = 0$, and $b$ is the boundary conditions for body sheet, i.e., $\eta \to \infty$. To achieve the convergence properties for the velocity, $f'(\eta)$, and temperature, $\theta(\eta)$, profiles, we set the tolerance limit of the model approximately to $10^{-6}$.

*2.4 Response Surface Methodology (RSM)*

To carry out the RSM analysis of heat transmission over the stretching/shrinking sheet, we use the procedures established by Yahaya *et al.,* and Samat *et al.,* [38,39]. The procedures are mentioned below:

i. Identify independent factor(s) and response(s);
ii. Develop a design of experimental (DOE) consists of (i);
iii. Formulate the prediction models using (i);
iv. Determine the optimal value of response(s).

The screening process for (i) includes choosing three independent factors that maximize two responses. The heat transfer coefficients for SWCNT-water and MWCNT-water nanofluids represent these responses.

In order to perform the RSM analysis with a sufficient number of simulation trials, we choose the second-order polynomial prediction model, as suggested previously by Husien *et al.,* [40]. Since we utilize the second-order polynomial prediction model, we express mathematically both SWCNT-water and MWCNT-water nanofluid prediction models using linear and quadratic terms. In addition, we conduct the RSM using the face-centered composite design (FCCD) method.

## 3. Results

*3.1 Code Validation*

To verify the accuracy of the programming code developed in section 2.3, we compare the data with the model of Bachok *et al*., [22]. The comparison data is based on the solution $f''(0)$ with the values of $\varepsilon = \phi = 0$. Because we have arrived at an excellent agreement with the previous model as displayed in Table 4, we are confident that we can proceed with the generation of solutions with varying key parameters in this model.

**Table 4**
Comparison data of $f''(0)$

| Bachok *et al*., [22] | Current model |
|---|---|
| 1.2326 | 1.2326 |

*3.2 Solutions $f''(0)$and $-\theta'(0)$*

In this section, we focus on determining the solutions $f''(0)$ and $-\theta'(0)$ due to the change in $\varepsilon$ and $M$. We vary $\varepsilon$ into two cases as follows:

i. $\varepsilon > 0$ is defined as the sheet with stretching velocity;
ii. $\varepsilon < 0$ is defined as the sheet with shrinking velocity.

To set the variation of $M$ and $\varepsilon$, we select $M = 0,0.02,0.04$ and $-2 \leq \varepsilon \leq 2$, respectively. In addition, we establish $Pr$ and $\phi$ at the constant values. We opt for a mixture of MWCNT and water as the main nanofluid in this section.

Based on the results in Figure 2 and Figure 3, we observe that the solutions $f''(0)$ and $-\theta'(0)$ consist of a single solution (the first solution) and multiple solutions (the first and second solutions). The single solution is produced in the stretching region, i.e., $\varepsilon > 0$, while the multiple solution is generated when the sheet is shrunk, i.e., $\varepsilon_c \leq \varepsilon < 0$. The term $\varepsilon_c$ in both Figure 2 and Figure 3 denote the critical point where the first and second solutions intersect. The creation of multiple solutions is advantageous in this model, as these solutions can be utilized to forecast flow separation resulting from variations in $M$. The postponement of flow separation caused by the presence of $M$ may suggest that the magnetic effect serves as a flow regulator, potentially benefiting various industries. According to Figure 2 and Figure 3, we also see that as the value of $M$ grows, the rate of flow detachment diminishes. Additionally, the increase in $M$ leads to an expansion of the solutions $f''(0)$ and $-\theta'(0)$.

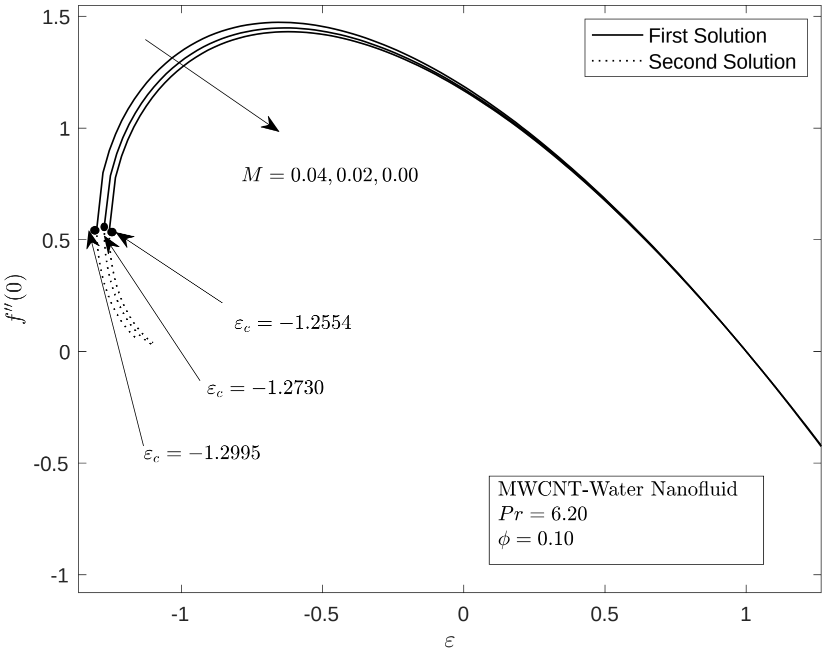


**Fig. 2.** Variation of solution $\boldsymbol{f''(0)}$ due to the changes in $\boldsymbol{M}$ and $\boldsymbol{\varepsilon}$

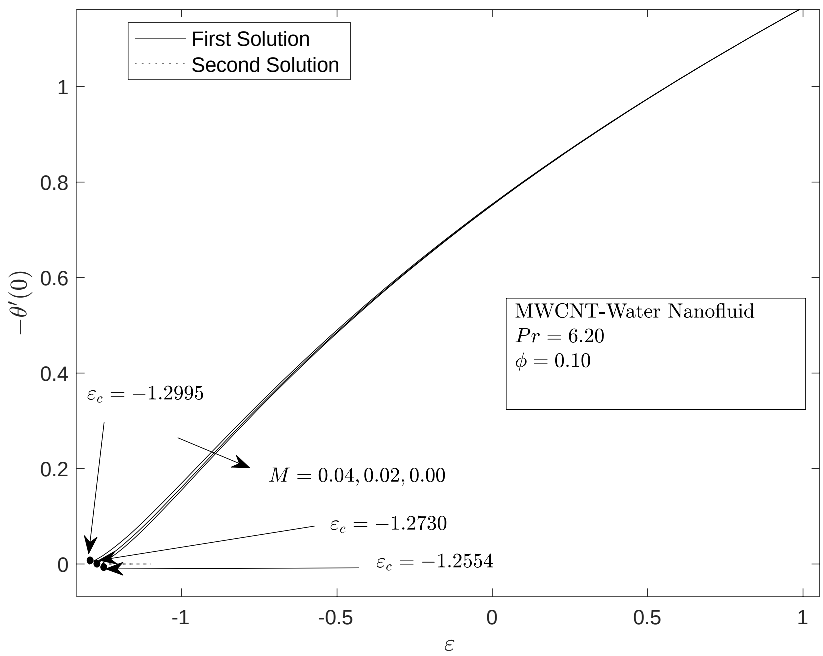


**Fig. 3.** Variation of solution $-\boldsymbol{\theta'(0)}$ due to the changes in $\boldsymbol{M}$ and $\boldsymbol{\varepsilon}$

### *3.3 Velocity and Temperature Profiles*

This section aims to visualize the velocity $f'(\eta)$, and temperature, $\theta(\eta)$, profiles. The profiles are depicted as a result of alterations in $M$ and $\eta$. We adjust the quantity of $M$ within the range of 0 to 0.02, while leaving $\eta$ grows up to a maximum of 15. In this numerical experiment, we choose SWCNT-water nanofluid by applying the constant values $Pr$, $\phi$, and $\varepsilon$, as indicated in Figure 4 and Figure 5.

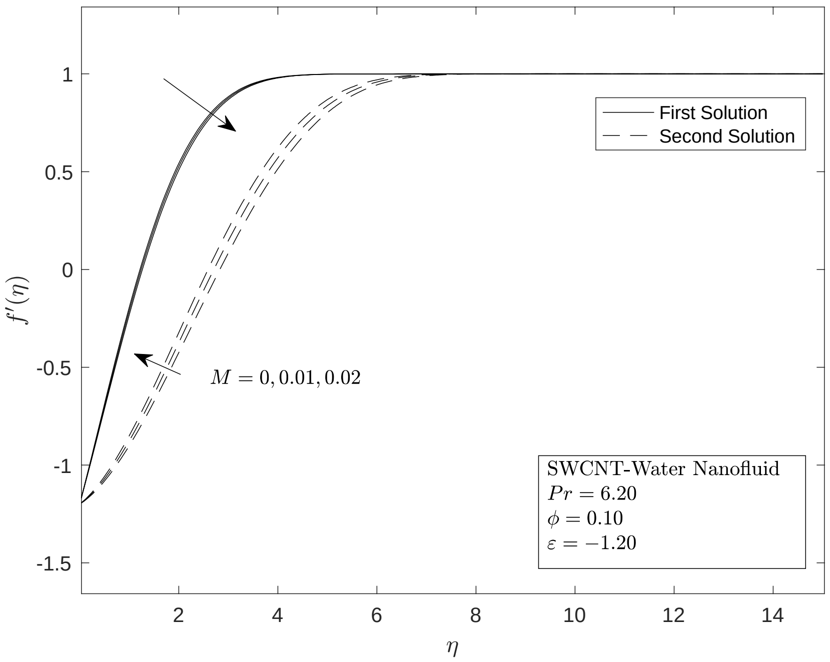


**Fig. 4.** Variation of velocity profile due to the changes in $\boldsymbol{M}$ and $\boldsymbol{\eta}$

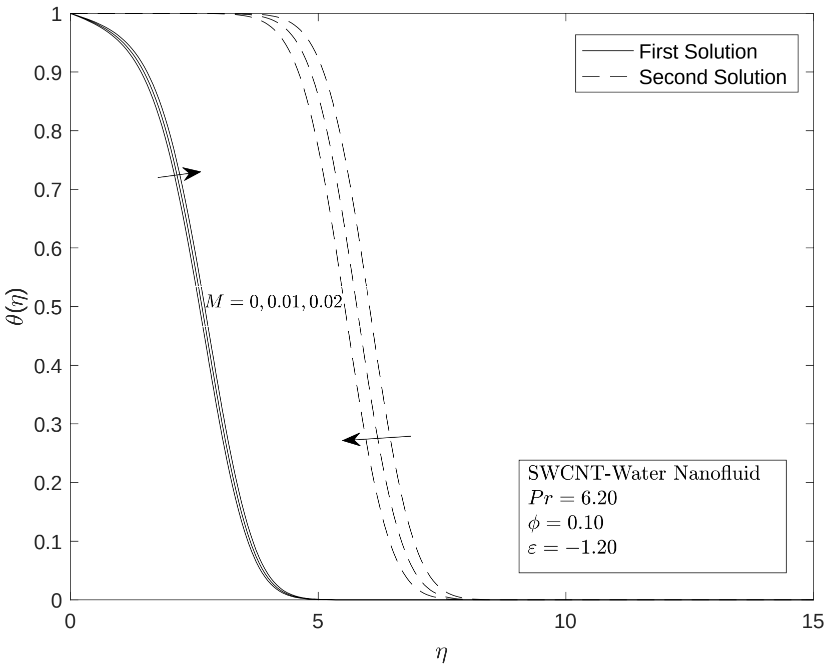


**Fig. 5.** Variation of temperature profile due to the changes in $M$ and $\eta$

The outcomes provided in Figure 4 and Figure 5 clearly demonstrate that both profiles adhere to the convergence properties established in the boundary conditions (Eqs. (9) to (10)). Furthermore, the first and second solutions tend to be upward trend for thermal and velocity profiles, respectively. According to Khatun and Islam [44], the magnetic field effect can influence the generation of the Lorentz force, which in turn has a positive effect on both profiles. The analysis of boundary layer thickness reveals that the second solution, as depicted in Figure 4 and Figure 5, is thicker than the first solution.

### *3.4 Skin Friction and Heat Transfer Coefficients*

To examine the variation of skin friction and heat transfer coefficients in response to alterations in different parameters, we intend to modify the value of $M$. Since the model is adapted from the Tiwari and Das model [32], we also take into account the variable value of $\phi$. The range of values of $M$ and $\phi$ are set at $M = 0.1, 0.2, 0.3$, while $0 \leq \phi \leq 0.1$. The other parameters are fixed unchanged at $Pr = 6.2$ and $\varepsilon = 0.5$. In addition, we employ both SWCNT-water and MWCNT-water nanofluids in order to evaluate their performance in terms of both coefficients. The comparison analysis between SWCNT-water and MWCNT-water nanofluids is conducted to provide engineers with insights for selecting the most effective CNT with optimal performance.

Based on the outcomes produced in Figure 6 and Figure 7, we can see that the positive impact for both coefficients is contributed due to the upward trends of $M$ and $\phi$. The rise in $M$ induces the strength of the Lorenz force, which leads to an increase in both coefficients. The findings presented in Figure 6 and Figure 7 corroborate the results previously obtained by Sahin and Namli [30] through experimental research. This team demonstrated that the heat transfer rate increased by up to 60% due to the sustained influence of the magnetic effect. The great influence of the magnetic field on both engineering interests potentially to be applied in real applications and devices. In addition, the growth in the value of $\phi$ increases the conductivity of both types of nanofluids, which contributes to the higher value of skin friction and heat transmission coefficients. The positive trend for both coefficients due to the rise in $\phi$ is contributed to by the excellent properties of CNT, particularly in thermal conductivity. However, in real practice, many applications should keep the volume fraction of CNT in low amounts to avoid the nanoparticle agglomeration problem. Omeiza *et al.,* [45] described that the agglomeration issue is one of the major difficulties in applying nanofluids in real applications. The findings in Figure 6 and Figure 7 also demonstrate that SWCNT-water nanofluid outperforms MWCNT-water nanofluid in terms of skin friction coefficient and heat transport through the stretching/shrinking sheet.

In this section, we also extend our investigation by assessing the performance of mono-nanofluid and hybrid nanofluid regarding the skin friction coefficient and transfer rate. We assume that the hybrid nanofluid is synthesized by mixing both SWCNT and MWCNT in water to create a hybrid SWCNT-MWCNT-water nanofluid. Based on our previous discovery of the excellent performance of SWCNT-water nanofluid in Figure 6 and Figure 7, we have selected this combination to represent a mono CNT nanofluid. Since this model prioritizes the magnetic effect, we vary the value of $M$ by altering it from $M = 0$ to $M = 1$. Meanwhile, we hold onto constant values for $Pr$, $\varepsilon$, and the volume fractions of mono-CNT and hybrid CNT. Visualization in Figure 8 and Figure 9 indicates that the hybrid CNT nanofluid excels the mono-CNT nanofluid in both coefficients. The exceptional effectiveness of the hybrid CNT nanofluid has fulfilled the potential for future research, as highlighted by Navrotskaya *et al.,* [46]. This team encourages researchers to enhance their understanding of hybrid CNT nanofluid flow behavior to broaden their applications in biological and ecological sectors.

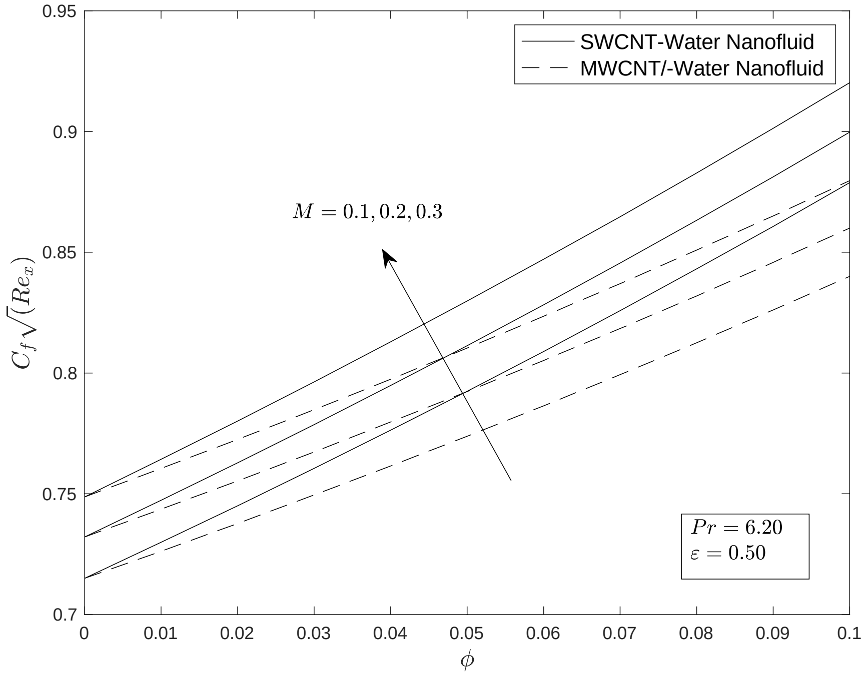


**Fig. 6.** Variation of skin friction coefficient due to the changes in $M$ and $\phi$

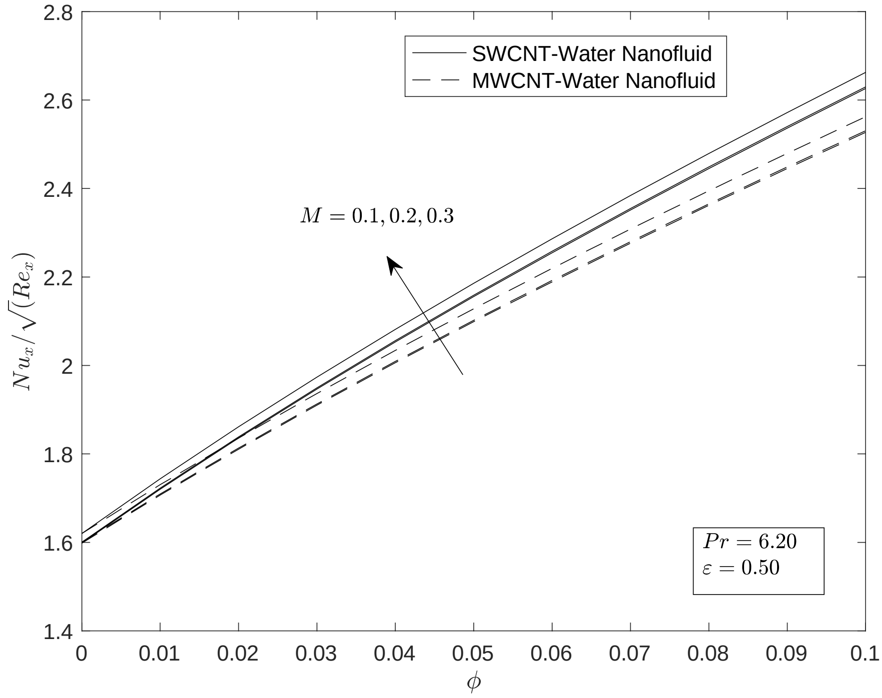


**Fig. 7.** Variation of heat transfer coefficient due to the changes in $M$ and $\phi$

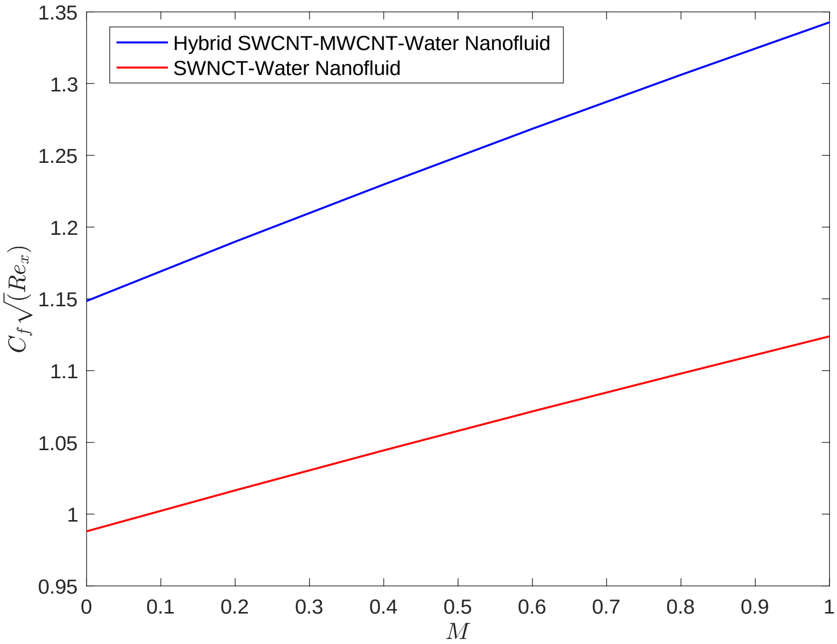


**Fig. 8.** Comparison between the mono-CNT and hybrid CNT nanofluids for skin friction coefficient due to the changes in $M$

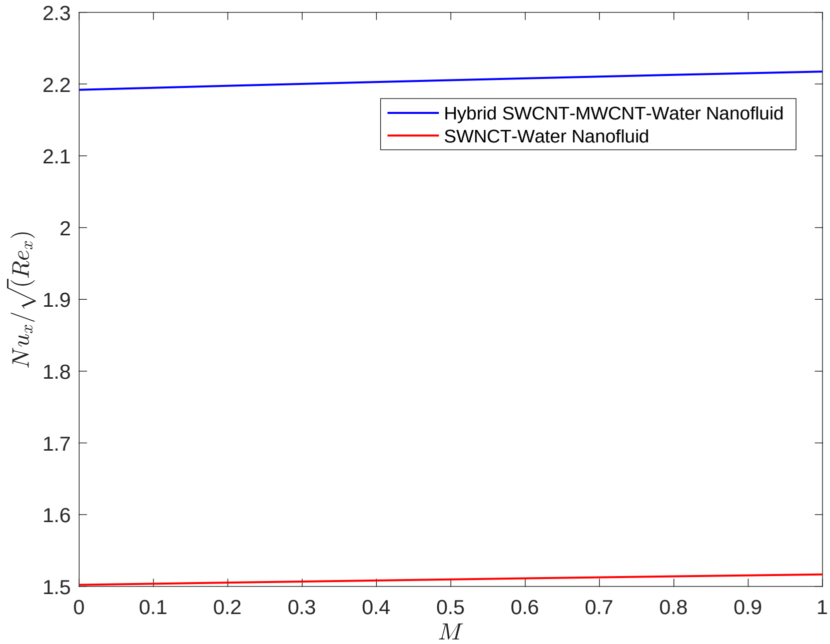


**Fig. 9.** Comparison between the mono-CNT and hybrid CNT nanofluids for heat transfer coefficient due to the changes in $M$

*3.5 Optimization of Heat Transfer Coefficient*

In this section, we develop the DOE for optimizing the heat transfer coefficient as required in Section 2.4. We display the DOE in Table 5 which consists of three main factors with their different limits. To select the factors, we select them based on Eqs (1) to (5) and the most significant parameter in the Tiwari and Das model [32].

**Table 5**
Factors that influence the heat transfer coefficient with their different limits

| Factor | Limit | | |
|---|---|---|---|
| | High $[+1]$ | Medium $[0]$ | Low $[-1]$ |
| Volume fraction of CNT, $\phi$ $[x_1]$ | 0.01 | 0.02 | 0.03 |
| Magnetic parameter, $M$ $[x_2]$ | 0.1 | 0.2 | 0.3 |
| Stretching parameter, $\varepsilon$ $[x_3]$ | 0.1 | 0.2 | 0.3 |

Note: The symbol [ ] indicates the coded parameter in Minitab

Next, by referring to the Yahaya *et al.,* model [38], we formulate the general quadratic model to predict the heat transfer coefficients for both SWCNT-water and MWCNT-water nanofluids. The models that consist of factors as in Table 5 are formulated below:

$$y_{SWCNT} = D_0 + D_1x_1 + D_2x_2 + D_3x_3 + D_{11}x_1^2 + D_{22}x_2^2 + D_{33}x_3^2 + D_{12}x_1x_2 + D_{13}x_1x_3 + D_{23}x_2x_3 + \epsilon_1, \quad (13)$$

and

$$y_{MWCNT} = E_0 + E_1x_1 + E_2x_2 + E_3x_3 + E_{11}x_1^2 + E_{22}x_2^2 + E_{33}x_3^2 + E_{12}x_1x_2 + E_{13}x_1x_3 + E_{23}x_2x_3 + \epsilon_2, \quad (14)$$

where $y_{SWCNT}$ and $y_{MWCNT}$ illustrate the heat transfer coefficients for SWCNT-water and MWCNT-water nanofluids, respectively. We provide the description of terms expressed in Eqs. (17) to (18) in Table 6.

**Table 6**
Description of terms in Eqs. (13) to (14)

| Term | Description |
|---|---|
| $D_0, E_0$ | Mean values |
| $D_1, D_2, D_3, E_1, E_2, E_3$ | Linear terms |
| $D_{11}, D_{22}, D_{33}, E_{11}, E_{22}, E_{33}$ | Quadratic terms |
| $D_{12}, D_{13}, D_{23}, E_{12}, E_{13}, E_{23}$ | Interaction terms |
| $\epsilon_1, \epsilon_2$ | Error terms |

To determine the number of trials for conducting the optimization process of the DOE in Minitab, we employ the following formula:

$$N = 2^F + 2F + C, \quad (15)$$

where $N$, $F$, and $C$ are the number of trials, factors, and center points, respectively. By replacing $F = 3$ and $C = 6$ in Eq. (15), we obtain $N = 20$. The arrangement of DOE with $N = 20$ can be viewed in Table 7.

**Table 7**
Design of experiment for the heat transfer coefficients of SWCNT-water and MWCNT-water nanofluids

| Run | Factor | | | Response | |
|---|---|---|---|---|---|
| | $[x_1]$ | $[x_2]$ | $[x_3]$ | $[y_{SWCNT}]$ | $[y_{MWCNT}]$ |
| 1 | $[-1]$ | $[-1]$ | $[-1]$ | 1.4014 | 1.3884 |
| 2 | $[+1]$ | $[-1]$ | $[-1]$ | 1.6100 | 1.5736 |
| 3 | $[-1]$ | $[+1]$ | $[-1]$ | 1.4107 | 1.3976 |
| 4 | $[+1]$ | $[+1]$ | $[-1]$ | 1.6204 | 1.5838 |
| 5 | $[-1]$ | $[-1]$ | $[+1]$ | 1.5770 | 1.5639 |
| 6 | $[+1]$ | $[-1]$ | $[+1]$ | 1.7963 | 1.7596 |
| 7 | $[-1]$ | $[+1]$ | $[+1]$ | 1.5834 | 1.5702 |
| 8 | $[+1]$ | $[+1]$ | $[+1]$ | 1.8035 | 1.7667 |
| 9 | $[-1]$ | [0] | [0] | 1.4943 | 1.4812 |
| 10 | $[+1]$ | [0] | [0] | 1.7087 | 1.6721 |
| 11 | [0] | $[-1]$ | [0] | 1.5995 | 1.5743 |
| 12 | [0] | $[+1]$ | [0] | 1.6078 | 1.5825 |
| 13 | [0] | [0] | $[-1]$ | 1.5128 | 1.4877 |
| 14 | [0] | [0] | $[+1]$ | 1.6924 | 1.6671 |
| 15 | [0] | [0] | [0] | 1.6037 | 1.5785 |
| 16 | [0] | [0] | [0] | 1.6037 | 1.5785 |
| 17 | [0] | [0] | [0] | 1.6037 | 1.5785 |
| 18 | [0] | [0] | [0] | 1.6037 | 1.5785 |
| 19 | [0] | [0] | [0] | 1.6037 | 1.5785 |
| 20 | [0] | [0] | [0] | 1.6037 | 1.5785 |

Analysis of variance (ANOVA) is applicable for evaluating the significance of the DOE, according to Chan *et al.,* [41]. The properties of ANOVA consist of the degree of freedom (DF), adjusted sum of squares (Adj SS), adjusted mean square (Adj MS), $F$-value and $p$-value. By depending on $p$-value, Mahanthesh *et al.,* and Samat *et al.,* [42,43] determined that a model is statistically significance if $p$-value is less than $0.05$. As displayed in Table 8, all sources for the ANOVA finding in $y_{SWCNT}$ exhibit significant terms, with the $p$-value $< 0.05$, except for the term $x_2^2$. Interestingly, in Table 9, we observe that the ANOVA outcome for $y_{MWCNT}$classifies all sources as significant elements.

**Table 8**
ANOVA result for the full model of heat transfer coefficient of SWCNT-water nanofluid

| Source | DF | Adj SS | Adj MS | $F$-Value | $p$-Value |
|---|---|---|---|---|---|
| Model | 9 | 0.195734 | 0.021748 | 9036111.08 | 0.000 |
| Linear | 3 | 0.195628 | 0.065209 | 27093533.35 | 0.000 |
| $x_1$ | 1 | 0.114940 | 0.114940 | 47755930.16 | 0.000 |
| $x_2$ | 1 | 0.000173 | 0.000173 | 71902.40 | 0.000 |
| $x_3$ | 1 | 0.080515 | 0.080515 | 33452767.48 | 0.000 |
| Square | 3 | 0.000046 | 0.000015 | 6385.77 | 0.000 |
| $x_1^2$ | 1 | 0.000013 | 0.000013 | 5553.00 | 0.000 |
| $x_2^2$ | 1 | 0.000000 | 0.000000 | 3.40 | 0.095 |
| $x_3^2$ | 1 | 0.000003 | 0.000003 | 1393.98 | 0.000 |
| 2-Way Interaction | 3 | 0.000061 | 0.000020 | 8414.12 | 0.000 |
| $x_1x_2$ | 1 | 0.000000 | 0.000000 | 187.49 | 0.000 |
| $x_1x_3$ | 1 | 0.000056 | 0.000056 | 23122.33 | 0.000 |
| $x_2x_3$ | 1 | 0.000005 | 0.000005 | 1932.53 | 0.000 |
| Error | 10 | 0.000000 | 0.000000 | | |
| Lack-of-Fit | 5 | 0.000000 | 0.000000 | | |
| Pure Error | 5 | 0.000000 | 0.000000 | | |
| Total | 19 | 0.195735 | | | |

**Table 9**
ANOVA result for the full model of heat transfer coefficient of MWCNT-water nanofluid

| Source | DF | Adj SS | Adj MS | $F$-Value | $p$-Value |
|---|---|---|---|---|---|
| Model | 9 | 0.171724 | 0.019080 | 13368463.58 | 0.000 |
| Linear | 3 | 0.171628 | 0.057209 | 40083070.72 | 0.000 |
| $x_1$ | 1 | 0.091107 | 0.091107 | 63832947.45 | 0.000 |
| $x_2$ | 1 | 0.000168 | 0.000168 | 117777.07 | 0.000 |
| $x_3$ | 1 | 0.080353 | 0.080353 | 56298487.64 | 0.000 |
| Square | 3 | 0.000037 | 0.000012 | 8544.32 | 0.000 |
| $x_1^2$ | 1 | 0.000009 | 0.000009 | 6529.66 | 0.000 |
| $x_2^2$ | 1 | 0.000000 | 0.000000 | 15.92 | 0.003 |
| $x_3^2$ | 1 | 0.000003 | 0.000003 | 2292.99 | 0.000 |
| 2-Way Interaction | 3 | 0.000059 | 0.000020 | 13775.69 | 0.000 |
| $x_1x_2$ | 1 | 0.000000 | 0.000000 | 283.76 | 0.000 |
| $x_1x_3$ | 1 | 0.000054 | 0.000054 | 37890.45 | 0.000 |
| $x_2x_3$ | 1 | 0.000004 | 0.000004 | 3152.87 | 0.000 |
| Error | 10 | 0.000000 | 0.000000 | | |
| Lack-of-Fit | 5 | 0.000000 | 0.000000 | | |
| Pure Error | 5 | 0.000000 | 0.019080 | | |
| Total | 19 | 0.171724 | | | |

Because the term $x_2^2$ in Table 8 possesses the $p$-value $> 0.05$, we remove this term from Table 8. The elimination of the term $x_2^2$ in Table 8 produces the reduced model for $y_{SWCNT}$. We demonstrate the ANOVA result for the reduced model for $y_{SWCNT}$ in Table 10. Given the presence of significant sources in the ANOVA results presented in Table 9 and Table 10, we can develop comprehensive prediction models for both $y_{SWCNT}$ and $y_{MWCNT}$. The mathematical formulations of these prediction models can be viewed in Eqs. (20) to (21).

**Table 10**
ANOVA result for the reduced model of heat transfer coefficient of SWCNT-water nanofluid

| Source | DF | Adj SS | Adj MS | $F$-Value | $p$-Value |
|---|---|---|---|---|---|
| Model | 8 | 0.195734 | 0.024467 | 8345268.52 | 0.000 |
| Linear | 3 | 0.195628 | 0.065209 | 22241900.63 | 0.000 |
| $x_1$ | 1 | 0.114940 | 0.114940 | 39204286.85 | 0.000 |
| $x_2$ | 1 | 0.000173 | 0.000173 | 59026.85 | 0.000 |
| $x_3$ | 1 | 0.080515 | 0.080515 | 27462388.19 | 0.000 |
| Square | 2 | 0.000046 | 0.000023 | 7862.02 | 0.000 |
| $x_1^2$ | 1 | 0.000016 | 0.000016 | 5403.47 | 0.000 |
| $x_3^2$ | 1 | 0.000004 | 0.000004 | 1381.40 | 0.000 |
| 2-Way Interaction | 3 | 0.000061 | 0.000020 | 6907.40 | 0.000 |
| $x_1x_2$ | 1 | 0.000000 | 0.000000 | 153.91 | 0.000 |
| $x_1x_3$ | 1 | 0.000056 | 0.000056 | 18981.82 | 0.000 |
| $x_2x_3$ | 1 | 0.000005 | 0.000005 | 1586.47 | 0.000 |
| Error | 11 | 0.000000 | 0.000000 | | |
| Lack-of-Fit | 6 | 0.000000 | 0.000000 | | |
| Pure Error | 5 | 0.000000 | 0.000000 | | |
| Total | 19 | 0.195735 | | | |

$$\begin{aligned} y_{SWCNT} = {} & 1.60369 + 0.107210x_1 + 0.004160x_2 + 0.089730x_3 - 0.002225x_1^2 \\ & - 0.001125x_3^2 + 0.000238x_1x_2 + 0.002638x_1x_3 + -0.000762x_2x_3, \end{aligned} \tag{16}$$

and

$$y_{MWCNT} = 1.57850 + 0.095450x_1 + 0.004100x_2 + 0.089640x_3 - 0.001841x_1^2 - 0.000091x_2^2 - 0.001091x_3^2 + 0.000225x_1x_2 + 0.002600x_1x_3 - 0.000750x_2x_3. \quad (17)$$

After developing the complete prediction models for both SWCNT-water and MWCNT-water, which incorporate statistically important variables as illustrated in Eqs. (20) to (21), we can proceed to identify the optimal solutions for each model. The optimal process is conducted using the response optimizer in Minitab. The outcomes of optimal solutions for both $y_{SWCNT}$ and $y_{MWCNT}$ are depicted in Table 11. With both models portraying $100\%$ composite desirability values, the maximum heat transfer coefficients for both models arrive at the highest values of $\phi$, $M$, and $\varepsilon$. As shown in the numerical approach in Section 3.4, we also confirm that SWCNT-water nanofluid works better than MWCNT-water nanofluid at transporting heat along the stretching/shrinking sheet using RSM analysis.

**Table 11**
Optimal solutions for both $y_{SWCNT}$ and $y_{MWCNT}$

| Model | Factor $x_1$ | $x_2$ | $x_3$ | Composite desirability | Optimal solution |
|---|---|---|---|---|---|
| $y_{SWCNT}$<br>$y_{MWCNT}$ | [+1] | [+1] | [+1] | 1.0000 | 1.8036<br>1.7667 |

## 4. Conclusions

We have conducted research on the boundary-layer flow of CNT-water nanofluid through the stretching/shrinking sheet under the MHD effect. We perform the investigation by employing numerical and RSM approaches. We have arrived at the following conclusions:

i. If the sheet shrinks along the $x$-axis, the model generates multiple solutions.
ii. The enhancement of the magnetic parameter expands the solution range and delays flow separation.
iii. A boost in the volume fraction of CNT and magnetic parameters improves both skin friction and heat transfer coefficients.
iv. The optimal heat transfer coefficient for CNT-water nanofluid is attained at the greatest values of CNT volume fraction, magnetic, and stretching parameters.
v. Both numerical and RSM analyses confirm that SWCNT-water nanofluid outperforms MWCNT-water nanofluid in terms of heat transfer coefficient.

**Acknowledgement**
This research was funded by a grant from Universiti Putra Malaysia (GP-GPB 9784400) and Universiti Sultan Azlan Shah (Dana Khas Penyelidikan Universiti Sultan Azlan Shah)

## References

[1] Najiyah Safwa Khashi'Ie, Hamzah, Khairum Bin, Iskandar Waini, Nurul Amira Zainal, Sayed Kushairi Sayed Nordin, Abdul Rahman Mohd Kasim, and IoanPop. "Response surface methodology of the unsteady axisymmetric magnetic hybrid nanofluid flow subject to a shrinking disk." *Journal of Advanced Research in Applied Mechanics* 112, no. 1 (2024): 137-148. https://doi.org/10.37934/aram.112.1.137148
[2] Tahir Mehmood, Muhammad Ramzan, Fares Howari, Seifedine Kadry, and Yu-Ming Chu. "Application of response surface methodology on the nanofluid flow over a rotating disk with autocatalytic chemical reaction and entropy generation optimization." *Scientific Reports* 11 (2021): 4021 https://doi.org/10.1038/s41598-021-81755-x

[3] Sheikh, A., Mohd Faizal Ali Akhbar, Nur Zhahirah Mat Zaib, Shahrizan bin Jamaludin, Wan Nurdiyana Wan Mansor, Che Wan Mohd Noor Che Wan Othman, and Anuar Abu Bakar. "Optimizing combustion pressure in single-cylinder diesel engine with response surface methodology (rsm) using blended plastic oil and palm oil biodiesel." *Semarak International Journal of Applied Sciences and Engineering Technology*, 1, no. 1 (2024): 36-48. https://semarakilmu.com.my/journals/index.php/sijaset/article/view/9506

[4] Najiyah Safwa Khashi'ie, Mohd Fariduddin Mukhtar, Nurul Amira Zainal, Khairum Hamzah, Iskandar Waini, Abdul Rahman Mohd Kasim, and Ioan Pop. "Sensitivity Analysis of MHD Hybrid Nanofluid Flow over a Radially Shrinking Disk with Heat Generation". *Journal of Advanced Research in Fluid Mechanics and Thermal Sciences* 117, no. 2 (2024): 116-130. https://doi.org/10.37934/arfmts.117.2.116130

[5] Reji, Meega and Kumar, Rupak. "Response surface methodology (RSM): An overview to analyze multivariate data." *Indian Journal of Microbiology Research* 9 (2023): 241-248. https://doi.org/10.18231/j.ijmr.2022.042

[6] Kim, Jiyun, Do-Gun Kim, and Kyung Hwan Ryu. "Enhancing response surface methodology through coefficient clipping based on prior knowledge." *Processes* 11, no. 12 (2023): 3392. https://doi.org/10.3390/pr11123392

[7] Ibham Veza, Martin Spraggon, I.M. Rizwanul Fattah, Muhammad Idris. "Response surface methodology (RSM) for optimizing engine performance and emissions fueled with biofuel: Review of RSM for sustainability energy transition." *Results in Engineering* 18 (2023): 101213. https://doi.org/10.1016/j.rineng.2023.101213

[8] Akaje, W., and B. I Olajuwon. "Impacts of Nonlinear Thermal Radiation on A Stagnation Point of An Aligned MHD Casson Nanofluid Flow with Thompson and Troian Slip Boundary Condition. *Journal of Advanced Research in Experimental Fluid Mechanics and Heat Transfer* 6, no. 1 (2021): 1-15. https://akademiabaru.com/submit/index.php/arefmht/article/view/3911

[9] Samat, N. A. A., Bachok, N. and Arifin, N. M. "Duality Solutions in Boundary Layer Flow and Heat Transfer of SWCNTs-MWCNTs/Water Hybrid Nanofluids over a Vertical Thin Needle with Effect of Suction." In *International Conference on Computational Heat and Mass Transfer*, pp. 34-45. Cham: Springer Nature Switzerland, 2023. https://doi.org/10.1007/978-3-031-66609-4_4

[10] Yahaya, Rusya Iryanti, Norihan Md Arifin, Ioan Pop, Fadzilah Md Ali, and Siti Suzilliana Putri Mohamed Isa. "Flow and Heat Transfer Analysis of Hybrid Nanofluid over a Rotating Disk with a Uniform Shrinking Rate in the Radial Direction: Dual Solutions." *Semarak International Journal of Nanotechnology* 1, no. 1 (2024): 29-44.

[11] Merkin, John H., Ioan Pop, Yian Yian Lok, and Teodor Grosan. Similarity solutions for the boundary layer flow and heat transfer of viscous fluids, nanofluids, porous media, and micropolar fluids. Academic Press, 2021.

[12] Choi, S.U.S. and Eastman, Jeffrey. "Enhancing thermal conductivity of fluids with nanoparticles." *Proceedings of the ASME International Mechanical Engineering Congress and Exposition* 66 (1995).

[13] Sidik, N. A. C., Yazid, M. N. A. W. M., and Mamat, R. "Recent advancement of nanofluids in engine cooling system." *Renewable and Sustainable Energy Reviews* 75 (2016): 137-144. https://doi.org/10.1016/j.rser.2016.10.057

[14] Japar, W. M. A. A., Sidik, N. A. C., Aid, S. Ra., Asako, Y., and Ken, T. L. "A Comprehensive Review on Numerical and Experimental Study of Nanofluid Performance in Microchannel Heatsink (MCHS)." *Journal of Advanced Research in Fluid Mechanics and Thermal Sciences* 45, no. 1 (2018): 165-176. https://semarakilmu.com.my/journals/index.php/fluid_mechanics_thermal_sciences/article/view/2711

[15] Loon, Y. W. and Sidik, N. A. C. "A comprehensive review of recent progress of nanofluid in engineering application: Microchannel heat sink (MCHS)." *Journal of Advanced Research in Applied Sciences and Engineering Technology* 28, no. 2 (2022): 1-25. https://doi.org/10.37934/araset.28.2.125

[16] Aziz, A. , Sidik, N. A. C., Rahman, S., Asako, Y., and Yusof, S. N. A. "A review of passive methods in microchannel heat sink application through advanced geometric structure and nanofluids: Current advancements and challenges." *Nanotechnology Reviews* 9 (2020): 1192-1216. https://doi.org/10.1515/ntrev-2020-0094

[17] Zafar, Mudasar, Hamzah Sakidin, Mikhail Sheremet, Iskandar B. Dzulkarnain, Abida Hussain, Roslinda Nazar, Javed Akbar Khan, Muhammad Irfan, Zafar Said, Farkhanda Afzal, and Abdullah Al-Yaari. "Recent development and future prospective of Tiwari and Das mathematical model in nanofluid flow for different geometries: A review." *Processes* 11, no. 3 (2023): 834. https://doi.org/10.3390/pr11030834

[18] Khoswan, Ibrahim, Abdelrahim Abusafa, and Saad Odeh. "The effect of carbon nanotubes on the viscosity and surface tension of heat transfer fluids—A Review Paper" *Energies* 17, no. 22 (2024): 5584. https://doi.org/10.3390/en17225584

[19] Afrand, M. and Ranjbarzadeh, Ramin. "Hybrid nanofluids preparation method." *Hybrid Nanofluids for Convection Heat Transfer*, (2020): 49-99. https://doi.org/10.1016/B978-0-12-819280-1.00002-1

[20] Crane, L. J. "Flow past a stretching plate." *Journal of Applied Mathematics and Physics* 21 (1970): 645-647.

[21] Dachapally Swapna, Gurala Thirupathi, Kamatam Govardhan, Narender, G., Santoshi Misra, and Renuka, S. "MHD stagnation point flow of micropolar fluid over a stretching/ shrinking sheet." *CFD Letters* 16, no. 12 (2024): 113-127. https://doi.org/10.37934/cfdl.16.12.113127

[22] Bachok, Norfifah, Ishak, Anuar and Pop, Ioan. "Stagnation-point flow over a stretching/shrinking sheet in a nanofluid." *Nanoscale Research Letters* 6 (2011): 623. https://doi.org/10.1186/1556-276X-6-623
[23] Yashkun, Ubaidullah, Zaimi, Khairy, Abu Bakar, Nor Ashikin, and Ferdows, Mohammad. "Nanofluid stagnation-point flow using Tiwari and Das model over a stretching/shrinking sheet with suction and slip effects." *Journal of Advanced Research in Fluid Mechanics and Thermal Sciences* 70 (2020): 62-76. https://doi.org/10.37934/arfmts.70.1.6276.
[24] Mahabaleshwar, U.S., Maranna, T., Mishra, M., Hatami, M., and Bengt Sunden. "Radiation effect on stagnation point flow of Casson nanofluid past a stretching plate/cylinder." *Scientific Reports* 14 (2024): 1387. https://doi.org/10.1038/s41598-024-51963-2
[25] Norzawary, N. H. A., Bachok, N., and Ali, M. F. "Stagnation point flow over a stretching/shrinking sheet in a carbon nanotubes with suction/injection effects." *CFD Letters* 122 (2021): 106-114. https://akademiabaru.com/submit/index.php/cfdl/article/view/3217
[26] Mahabaleshwar, U. S., Sneha, K. N., and Huang-Nan Huang. "Newtonian flow over a porous stretching/shrinking sheet with CNTS and heat transfer." *Journal of the Taiwan Institute of Chemical Engineers* 134 (2022): 104298. https://doi.org/10.1016/j.jtice.2022.104298
[27] Mahabaleshwar, U. S., Sneha, K. N., Chan, A., and Dia Zeidan. "An effect of MHD fluid flow heat transfer using CNTs with thermal radiation and heat source/sink across a stretching/shrinking sheet." *International Communications in Heat and Mass Transfer* 135 (2022): 106080. https://doi.org/10.1016/j.icheatmasstransfer.2022.106080
[28] Samat, N. A. A., Bachok, N. and Arifin, N. M. "Carbon nanotubes (CNTs) nanofluids flow and heat transfer under mhd effect over a moving surface." *Journal of Advanced Research in Fluid Mechanics and Thermal Sciences* 103, no. 1 (2023): 165-178. https://doi.org/10.37934/arfmts.103.1.165178
[29] Kang, J., Al-Sabah, S., and Théo, R. "Effect of single-walled carbon nanotubes on strength properties of cement composites." *Materials* (*Basel*), (2020). https://doi.org/10.3390/ma13061305
[30] Sahin, Fevzi, and Lutfu Namli. "Experimental investigation of heat transfer characteristics of magnetic nanofluids (MNFs) under a specially designed revolving magnetic field effect." *Journal of Magnetism and Magnetic Materials* 580 (2023): 170961. https://doi.org/10.1016/j.jmmm.2023.170961
[31] Jaafar, A., Waini, I., Jamaludin, A., Nazar, R., and Pop, I. "MHD flow and heat transfer of a hybrid nanofluid past a nonlinear surface stretching/shrinking with effects of thermal radiation and suction." *Chinese Journal of Physics* 79 (2022): 13-27. https://doi.org/10.1016/j.cjph.2022.06.026
[32] Tiwari, R. K. and Das, M. K. "Heat Transfer Augmentation in a Two-Sided Lid-Driven Differentially Heated Square Cavity Utilizing Nanofluids." *International Journal Heat Mass Transfer* 50 (2007): 2002-2018. http://dx.doi.org/10.1016/j.ijheatmasstransfer.2006.09.034
[33] Samat, N. A. A., Bachok, N. and Arifin, N. M. "The significant effect of hydromagnetic on carbon nanotubes based nanofluids flow and heat transfer past a porous stretching/shrinking sheet." *Journal of Advanced Research in Fluid Mechanics and Thermal Sciences* 106, no. 1 (2023): 51-64. https://doi.org/10.37934/arfmts.106.1.5164
[34] Khan, Waqar and Pop, I. "Boundary-layer flow of a nanofluid past a stretching sheet." *International Journal of Heat and Mass Transfer* 53 (2010): 2477-2483. https://doi.org/10.1016/j.ijheatmasstransfer.2010.01.032
[35] Afzal, N., Badaruddin, A., and Elgarvi, A. A. "Momentum and Heat Transport on a Continuous Flat Surface Moving in a Parallel Stream." *International Journal of Heat and Mass Transfer* 36, no. 13 (1993): 3399-3403. https://doi.org/10.1016/0017-9310(93)90022-X
[36] Khan, W. A., Khan, Z. H., and Rahi, M. "Fluid flow and heat transfer of carbon nanotubes along a flat plate with Navier slip boundary". *Applied Nanoscience* 4 (2014): 633-641. https://doi.org/10.1007/s13204-013-0242-9
[37] Samat, N. A. A., Bachok, N., and Arifin, N. M. "Magnetohydrodynamic flow of carbon nanotubes and heat transfer over a moving thin Needle: A numerical and research surface methodology. *Ain Shams Engineering Journal* 15, no. 8 (2024): 102833. https://doi.org/10.1016/j.asej.2024.102833
[38] Yahaya, R. I., Mustafa, M. S., Arifin, N. M., Pop, I., Ali, F. M., and Isa, S. S. P. M. "Hybrid nanofluid flow past a biaxial stretching/shrinking permeable surface with radiation effect: Stability analysis and heat transfer optimization." *Chinese Journal of Physics* 85 (2023): 402-420. https://doi.org/10.1016/j.cjph.2023.06.003
[39] Samat, N. A. A., Bachok, N., and Arifin, N. M. "Hybrid carbon nanotubes flow and heat transfer over a vertical thin needle with suction effect: A numerical and optimisation analysis." *International Communications in Heat and Mass Transfer* 156 (2024): 107702. https://doi.org/10.1016/j.icheatmasstransfer.2024.107702
[40] Husien, S., El-taweel, R. M., Salim, A. I., Fahim, I. S., Said, L. A., and Radwan, A. G. "Review of activated carbon adsorbent material for textile dyes removal: Preparation, and modelling." *Current Research in Green and Sustainable Chemistry* 5 (2022): 100325. https://doi.org/10.1016/j.crgsc.2022.100325
[41] Chan, S. Q., Aman, F., and Mansur, S. "Bionanofluid flow through a moving surface adapting convective boundary condition: Sensitivity analysis." *Journal of Advanced Research in Fluid Mechanics and Thermal Sciences* 54, no. 1 (2019): 57-69.

[42] Mahanthesh, B., Shahzad, Sher, Mackolil, Joby, and Shashikumar, N. S. "Heat transfer optimization of hybrid nanomaterial using modified Buongiorno model: A sensitivity analysis." *International Journal of Heat and Mass Transfer* 171 (2021): 121081. https://doi.org/10.1016/j.ijheatmasstransfer.2021.121081

[43] Samat, N. A. A., Bachok, N., and Arifin, N. M. "Boundary layer stagnation point flow and heat transfer over a nonlinear stretching/shrinking sheet in hybrid carbon nanotubes: Numerical analysis and response surface methodology under the influence of magnetohydrodynamics." *Computation* 12, no. 3 (2024): 46. https://doi.org/10.3390/computation12030046

[44] Khatun, Mst Asiya, and Tarikul Islam. "Influence of magnetic field and heat generation/absorption on unsteady MHD convective flow along a permeable stretching/shrinking wedge with thermophoresis and variable fluid properties." *International Journal of Thermofluids* 16 (2022): 100204. https://doi.org/10.1016/j.ijft.2022.100204

[45] Omeiza, Lukman Ahmed, Muhammad Abid, Yathavan Subramanian, Anitha Dhanasekaran, Saifullah Abu Bakar, and Abul Kalam Azad. "Challenges, limitations, and applications of nanofluids in solar thermal collectors—a comprehensive review." *Environmental Science and Pollution Research* (2023): 1-29. https://doi.org/10.1007/s11356-023-30656-9

[46] Navrotskaya, A. G., Aleksandrova, D. D , Krivoshapkina, E. F., Sillanpää, M., and Krivoshapkin, P. V. "Hybrid materials based on carbon nanotubes and nanofibers for environmental applications." *Front Chem*. 8 (2020): 546. https://doi.org/10.3389/fchem.2020.00546